Ultra Shallow Seismic Reflection in Unconsolidated Sediments: Rock Physics base for data acquisition.

Ran Bachrach and Amos Nur, Stanford University*

Summary

Typical high-resolution shallow seismic methods target depths of < 500m. However, obtaining high-resolution seismic reflection images of depths shallower than 5-10m is often assumed not to be possible. There is still a great need to better understand the seismic response of the near surface.

In this paper we address the problem of ultra-shallow seismic acquisition in unconsolidated sediments. We show that the velocity profile in the upper few meters of unconsolidated sediments is pressure dependent, and the very near surface P- and S-wave velocities are very low. We show that, given this velocity profile, groundroll will be attenuated greatly by scattering attenuation in the presence of very mild surface roughness. This attenuation of the high frequencies of the groundroll causes the separation of the reflection energy from the groundroll energy in the frequency domain. This separation enables us to image seismic reflections very near the surface. We present field examples from three different locations where we were able to obtain very shallow reflections (1-3m) in unconsolidated sediments.

Introduction

Ultra-shallow seismic acquisition is an underdeveloped field (Steeples *et al*. 1997). Typically, high-resolution shallow seismic reflection survey target reflections in the "Optimum" window range (Hunter *at al.*, 1984), defined as the zone between the first arrivals and the groundroll (Fig. 1). In this zone, the reflections are not contaminated by the groundroll and can be easily imaged. However, using the optimum window technique does not allow for very short offsets, and therefore typically shallow reflections arriving at times earlier than 35-50ms are difficult to image. Hence, using only the optimum window limits the reflection profile to depths of more than 5-10m. Furthermore, for ultra-shallow imaging, one must obtain the reflections inside the groundroll.

The attenuation of groundroll is typically done using geophone arrays or frequency filtering. Geophone arrays are not very useful in ultra-shallow reflection surveys because the dimensions of such arrays are typically larger than the required station spacing. Therefore, frequency filtering is the only effective tool for attenuating groundroll. The ability to obtain shallow reflections depends on the separation of groundroll from reflected energy in the frequency domain. In this paper we show that in unconsolidated sediments, where velocities are pressure dependent, this separation can be achieved.

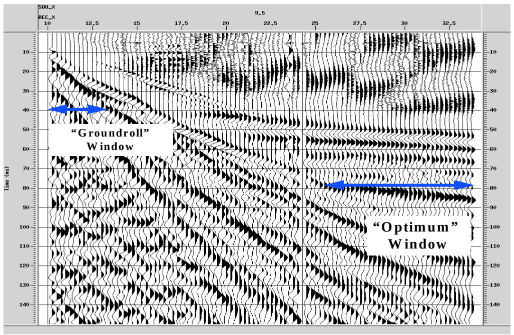

Fig. 1. The optimum window and groundroll window in shallow shot gather.

Velocity Profile in Shallow Unconsolidated Sediments

Velocities in unconsolidated sediments are governed by the overburden pressure. Recently, Bachrach *et al*. showed that the pressure dependent P- and S- wave velocity-versus-pressure profiles in sands can be modeled based on contact mechanics (Bachrach *et al*., 1998a, and 1998b). The functional dependence of the velocity-depth profile in general is related to the grain elastic moduli, density, shape, the porosity etc.. In unconsolidated sediments, the top layer of grains is a suspension of grains in air, and the elastic stiffness increase with depth is due to the overburden pressure effect on contact stiffness. This dependence is given in equations (1) and (2). (A more detailed discussion on these results is given in Bachrach *et al*, 1998b).

$$G_C = \alpha_G Z^{\frac{1}{6}}, \quad K_C = \alpha_K Z^{\frac{1}{6}}$$
$$\frac{1}{K_U} = \frac{1}{K_C} + \phi/(K_0 + \frac{K_0 K_{air}}{K_0 - K_{air}}), \quad G_U = G_C \tag{1}$$

where K_U and G_U are bulk and shear moduli of the sediment, Z is depth, ϕ is porosity, K_0 is the grain modulus, K_{air} is the air bulk modulus, and α_G and α_K are constants which in general are functions of all the other sediment parameters, and can be determined experimentally. The effective bulk and shear moduli in vacuum are given by K_C and G_C respectively.

The P- and S-wave velocities are given by:

$$V_p = \sqrt{\frac{K_U + \frac{4}{3}G_U}{\rho}}, \quad V_s = \sqrt{\frac{G_U}{\rho}} \qquad (2)$$

where ρ is the bulk density of the sediment.

The P- and S-wave velocities in unconsolidated sand (Fig. 2) show that the velocity gradient is very steep in the very near surface, and the P and S wave velocities at the surface are very low. We will show below that this fact causes separation of groundroll energy from the reflected energy.

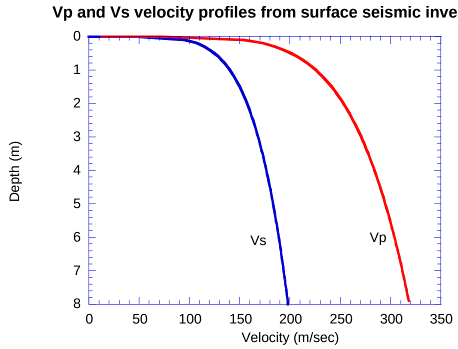

Fig. 2 Velocity profiles in shallow unconsolidated sand. This profile is typical of unconsolidated sediments with pressure dependent velocity.

Imaging Inside the Groundroll in Unconsolidated Sediments: Field Observations

Figure 3a presents a shot gather collected on beach sand together with its power spectrum. Reflections in the gather at the very top part of the seismogram are masked by the surface waves, seen here as the low velocity waves propagating in a steep angle along the seismogram. Figure 3b presents the same seismic section after frequency filtering. Note that there are clear reflections at 20 and 10ms, which were not visible before. In Fig. 4 we show two more shot gathers from two different environments: A river sandbar (A,B) and soil over bedrock (C,D). Note that the very shallow reflections can be seen in all shot gathers inside the groundroll window after low-cut filtering. Again, there is a good separation in the frequency domain between groundroll and reflections. Note also that the velocities in all three shot records are very low (slower than the airwave). Thus the attenuation of the groundroll in very short offsets is common in all of these cases.

It is known from theory that the Rayleigh waves are non-dispersive in a homogenous elastic medium. The question then is: why is there such a separation in the frequency domain between groundroll and the shallow reflections? What is the physical reason that enables us to suppress the groundroll and yet retain the reflections?

To answer this question, we will go back to the basic attenuation mechanism of groundroll. We will limit the discussion to Rayleigh waves.

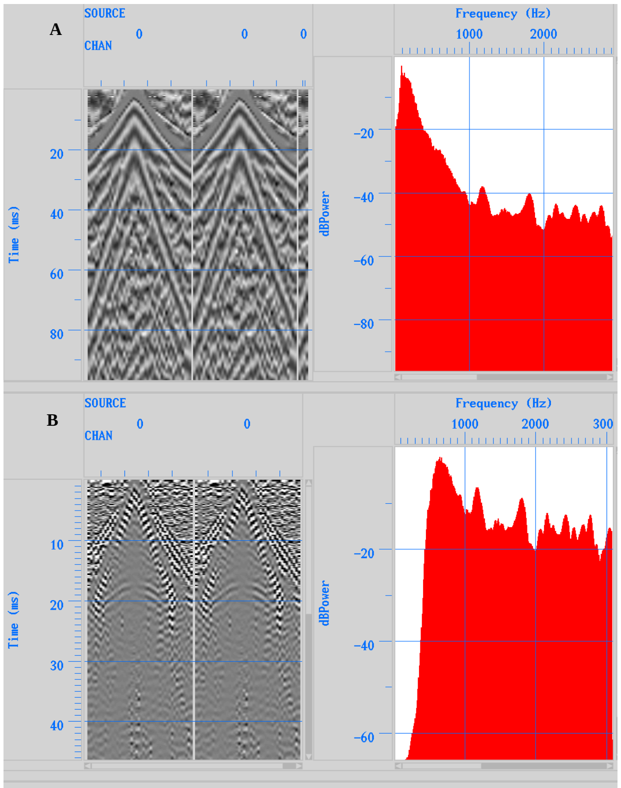

Fig. 3: Power spectrum of a shot gather: A. Raw data (acquired with 40Hz Geophones) B. Same gather after low cut filtering of 700Hz. The reflections are clearly visible inside the groundroll zone due to a good separation between groundroll and reflection energy in the frequency domain.

The Attenuation of Rayleigh Surface Waves due to Surface Roughness in Low-Velocity Unconsolidated Sediments

The attenuation of surface waves depends on two main factors: (1). energy loss per unit cycle due to viscoelastic and inelastic effects, and (2). scattering attenuation. We show next that, in unconsolidated sediments, the separation of reflected wave energy from the Rayleigh wave energy in the frequency domain is expected and is caused mainly by the scattering attenuation of the surface wave from the surface roughness.

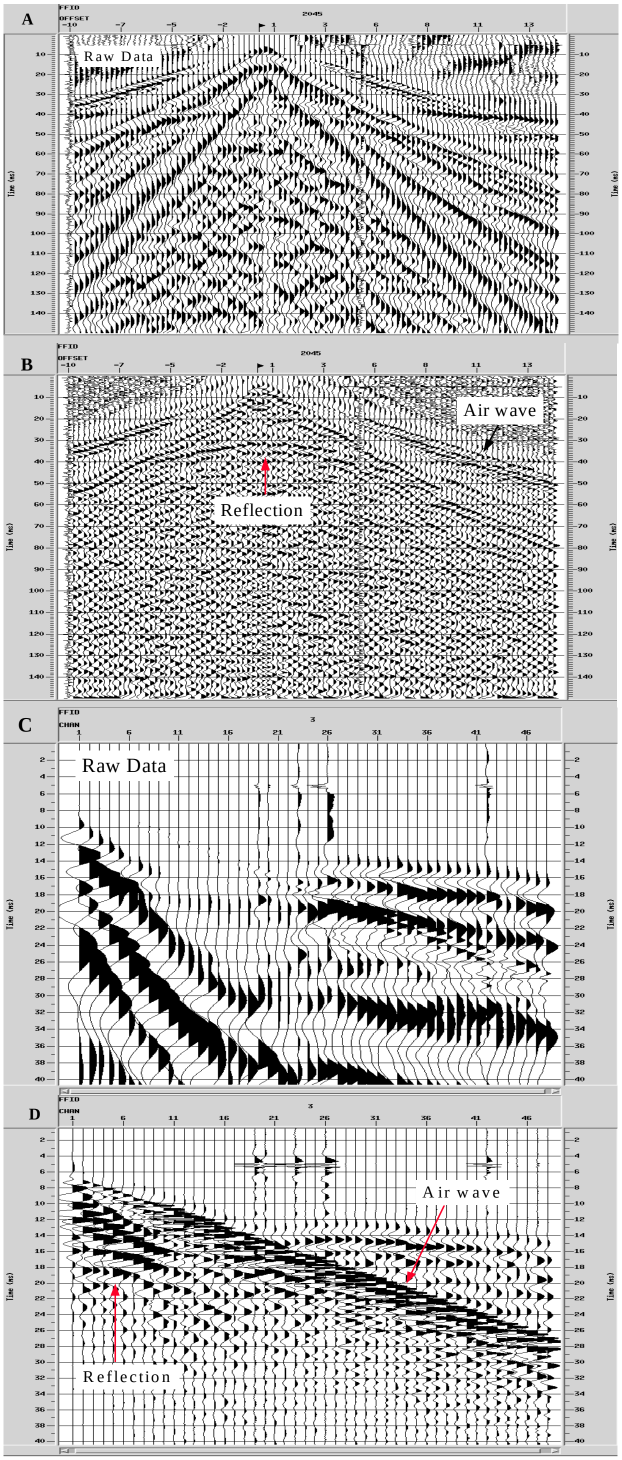

Fig. 4 Data from different geological environments A. Raw data from a river sand bar. B. same as A but with 300Hz lowcut. C. Raw data from Soil over bedrock. D. same as C but with 500Hz. low cut filter.

The attenuation of Rayleigh surface waves due to surface roughness was studied in detail by Maradudin and Mills, (1976). They used Green's function approach together with Born approximation to derive the energy loss per unit distance for a Rayleigh wave scattering from surface roughness. This energy loss per unit distance is expressed as attenuation length β. Maradudin and Mills showed that for a Gaussian surface roughness with correlation length a and RMS amplitude δ the attenuation length can be approximated by the expression:

$$\beta = \alpha_0 f(a\omega / V_R)$$

where

$$\alpha_0 = \frac{\delta^2 a^2 \omega^5}{\pi V_R^5},$$

$$f(a\omega/V_R) \cong \frac{\pi^2}{R^2}\left(\frac{V_R}{V_S}\right)^4 \left(1-\frac{1}{2}\frac{V_R{}^2}{V_S{}^2}\right)^{-2} \left(1-\frac{V_R{}^2}{V_P{}^2}\right)^{-1}$$

$$\times\left[\left(1-\frac{V_S{}^2}{V_P{}^2}\right)\left(\frac{1}{2}-\frac{V_S{}^2}{V_P{}^2}\right)\right]+\frac{1}{32}, \qquad \frac{a\omega}{V_R} \ll 1 \qquad (3)$$

$$\times\left[\left(1-\frac{V_S{}^2}{V_P{}^2}\right)^2 \frac{V_R}{\pi^{1/2} a\omega}\right], \qquad \frac{a\omega}{V_R} \gg 1$$

V_P, V_S and V_R are the P-, S- and Rayleigh- wave velocities in the sediment, respectively, and ω is the angular frequency. [The complete expression can be found in Maradudin and Mills, (1976)].

For most unconsolidated sediments with Poisson ratio of 0.1-0.2, the Rayleigh wave velocity is $V_R \cong 0.9 V_S$ Note also that β is related to the amplitude of the surface roughness squared (δ^2), the correlation length squared (a^2), and the Rayleigh wavelength to the power of (-5) (λ_R^{-5}). The attenuation length β is plotted as a function of different surface roughness amplitude and different shear wave velocities in Fig. 5. Fig. 6 shows a 300Hz wavelet transmitted in a medium which has 0.5m correlation length and δ of 2cm. Note that in the low velocity material the wavelet is almost totally attenuated. Note also that for higher velocities, the attenuation coefficient is much smaller.

Conclusions

We have shown that ultra-shallow seismic reflections can be obtained if they can be separated from the groundroll that masks these events in the very short offset part of the seismogram. We have also shown that the velocity profile in shallow, unconsolidated sand causes the surface wave velocity, and hence wavelength, to be very small. Thus the effect of even mild surface roughness (say 2cm height), is significant for the attenuation of the surface wave even at very short offsets.

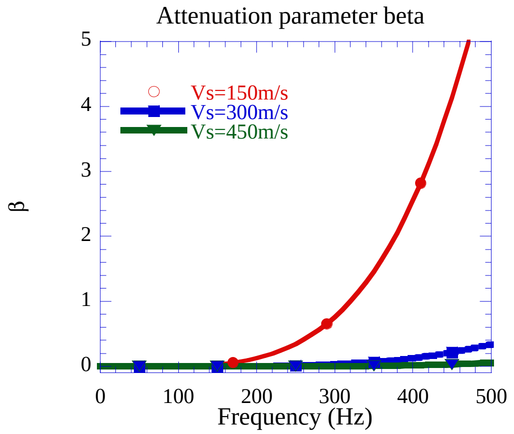

Fig. 5 Attenuation parameter for 3 different media with V_P and V_S of: (A). 240m/s and 150m/s, (B). 480m/s and 300m/s, and (C). 720m/s and 450m/s.

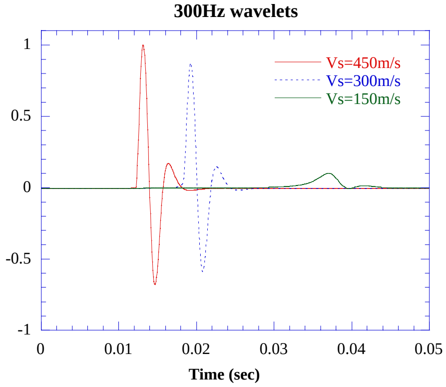

Fig 6 300Hz waveforms propagating 5m distance in the three different media in Fig 5. Note that the low velocity wavelet is completely attenuated and has lost all of its high frequencies. Thus, a good separation in the frequency domain is expected for materials with such low velocities, e.g. unconsolidated sediments.

In our numerical example, a 300Hz wavelet was critically damped within less than 5m propagation length in a material with V_P and V_S of 240m/s and 150m/s respectively. We note that the actual attenuation of the high-frequency surface wave is not a function of the velocity alone, but has other parameters which affect it (such as correlation length, surface roughness distribution and other attenuation mechanisms). Some of these surface parameters are difficult to estimate. However, the near surface velocity profile in unconsolidated materials is constrained. Thus, the wavelength of the groundroll at high frequencies is small and will always be more attenuated than the reflected wave. The reflection energy can be separated from the groundroll, as we observed in our experiments.

Acknowledgements

This work was supported by the Stanford Rock Physics project. We thank Dr. Tapan Mukerji for valuable discussions.

References

Bachrach, R., 1998, High resolution shallow seismic experiments in sand: 2). Velocities in shallow unconsolidated sands, Geophysics, In press.

Bachrach, R., J. Dvorkin,. and A. Nur., 1998, Elasticity of shallow, unconsolidated sediments, In preparation.

Hunter, J. A., S. E. Pullan, R. A. Burns, R. Gagne, and R. Good, 1984, Shallow reflection mapping of the overburden bedrock interface with engineering seismograph- Some simple techniques, Geophysics, **49**, 1381-1385.

Maradudin, A. A., and D. L. Mills, 1976, The attenuation of Rayleigh surface waves by surface roughness, Annals of Physics, **1000**, 262-309.

Steepls, D., W., A. G. Green, T. V. McEvilly, R. D. Miller, W. E. Doll, and J. W. Rector, 1997, A workshop examination of shallow seismic reflection surveying, The Leading Edge, **16**, 1641-1647.